Leukemia (2020) 34:2964–2980
https://doi.org/10.1038/s41375-020-0754-8

ARTICLE

Lymphoma

The novel lncRNA BlackMamba controls the neoplastic phenotype of ALK⁻ anaplastic large cell lymphoma by regulating the DNA helicase HELLS

Valentina Fragliasso[1] · Akanksha Verma[2,3] · Gloria Manzotti[1] · Annalisa Tameni[1,4] · Rohan Bareja[2] · Tayla B. Heavican[5] · Javeed Iqbal[5] · Rui Wang[6] · Danilo Fiore[6] · Valentina Mularoni[1] · Wing C. Chan[7] · Priscillia Lhoumaud[8] · Jane Skok[8] · Eleonora Zanetti[9] · Francesco Merli[10] · Alessia Ciarrocchi[1] · Oliver Elemento[2] · Giorgio Inghirami[6]

Received: 7 August 2019 / Revised: 20 January 2020 / Accepted: 10 February 2020 / Published online: 2 March 2020

Abstract

The molecular mechanisms leading to the transformation of anaplastic lymphoma kinase negative (ALK⁻) anaplastic large cell lymphoma (ALCL) have been only in part elucidated. To identify new culprits which promote and drive ALCL, we performed a total transcriptome sequencing and discovered 1208 previously unknown intergenic long noncoding RNAs (lncRNAs), including 18 lncRNAs preferentially expressed in ALCL. We selected an unknown lncRNA, *BlackMamba*, with an ALK⁻ ALCL preferential expression, for molecular and functional studies. *BlackMamba* is a chromatin-associated lncRNA regulated by STAT3 via a canonical transcriptional signaling pathway. Knockdown experiments demonstrated that *BlackMamba* contributes to the pathogenesis of ALCL regulating cell growth and cell morphology. Mechanistically, *BlackMamba* interacts with the DNA helicase HELLS controlling its recruitment to the promoter regions of cell-architecture-related genes, fostering their expression. Collectively, these findings provide evidence of a previously unknown tumorigenic role of STAT3 via a lncRNA-DNA helicase axis and reveal an undiscovered role for lncRNA in the maintenance of the neoplastic phenotype of ALK⁻ALCL.

Introduction

Peripheral T-cell lymphomas (PTCLs) are a heterogeneous group of tumors, which include 29 different subtypes according to the World Health Organization (WHO). Among them, systemic CD30-positive anaplastic large cell

Supplementary information The online version of this article (https://doi.org/10.1038/s41375-020-0754-8) contains supplementary material, which is available to authorized users.

✉ Alessia Ciarrocchi
alessia.ciarrocchi@ausl.re.it

✉ Oliver Elemento
ole2001@med.cornell.edu

✉ Giorgio Inghirami
ggi9001@med.cornell.edu

[1] Laboratory of Translational Research, Azienda USL-IRCCS di Reggio Emilia, Reggio Emilia 42123, Italy

[2] Institute for Computational Biomedicine & Caryl and Israel Englander Institute for Precision Medicine, Weill Cornell Medicine, New York, NY 10021, USA

[3] Tri-Institutional Training Program in Computational Biology and Medicine, New York, NY 10065, USA

[4] Clinical and Experimental Medicine PhD Program, University of Modena and Reggio Emilia, Modena 41125, Italy

[5] Pathology and Microbiology, University of Nebraska Medical Center, Omaha, NE 68182, USA

[6] Department of Pathology and Laboratory Medicine, Weill Cornell Medicine, New York, NY 10065, USA

[7] Department of Pathology, City of Hope National Medical Center, Duarte, CA 91010, USA

[8] Department of Pathology, New York University School of Medicine, Langone Medical Center, New York, NY 10016, USA

[9] Pathology Unit, Azienda USL-IRCCS di Reggio Emilia, Reggio Emilia 42123, Italy

[10] Hematology Unit, Azienda USL-IRCCS di Reggio Emilia, Reggio Emilia 42123, Italy

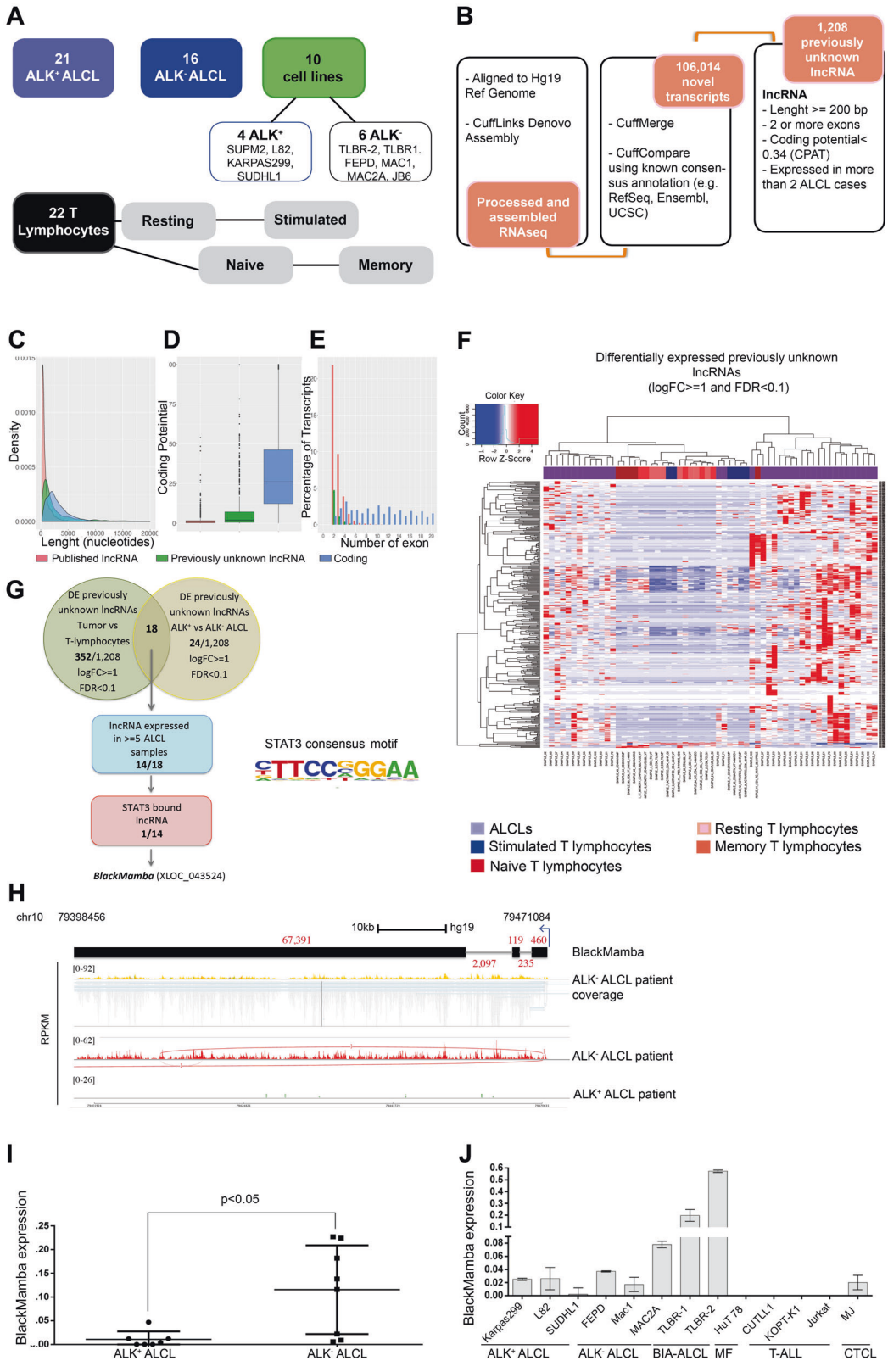

lymphomas (ALCL) are characterized by distinct histopathological and clinical features. ALCL are stratified based on the presence of anaplastic lymphoma kinase (*ALK*) translocations [1–4]. Clinically, systemic ALK⁻ALCL displays a poor response to therapy and inferior survival compared with ALK⁺ALCL [4–9]. Within ALK⁻ALCL,

◀ **Fig. 1 ALCL samples expressed a restricted set of aberrantly activated previously unknown lncRNAs. a** Schematic representation of human samples used to perform directional RNA sequencing. **b** Bioinformatic pipeline for the discovery of previously unknown lncRNAs. **c** Density plot for transcript length shows shared pattern between previously unknown and known lncRNAs compared with protein-coding genes, which are much longer. **d** Coding Potential Score obtained from GENEID shows that previously unknown lncRNAs and known lncRNAs have comparable and lower average coding potential than do protein-coding genes. **e** Comparing previously unknown lncRNAs against all transcripts with at least two or more exons show a greater number of exons for the protein-coding genes. **f** Unsupervised analysis of previously unknown lncRNAs profile across normal T-cell lymphocytes and ALCL primary samples. **g** Flowchart for the discovery of *BlackMamba* in ALK$^-$ ALCL samples. **h** Schematic representation of locus, structure, and aligned reads of *BlackMamba*. Numbers represent the length (bp) of exons and introns (gray). Sashimi plots of representative ALK$^-$ and AL$^+$ ALCL samples were generated by Integrative Genomics Viewer software. The genomic coordinates are measured along the horizontal axis and the RPKM (Reads Per Kilobase per Million mapped reads) values up the vertical axis. qRT-PCR analysis of *BlackMamba* in a validation set of ALCLs samples (**i**) and in a panel of cell lines (**j**).

distinct subsets have been described [7]. ALK$^-$ALCL share unique transcriptional signatures [6, 10] and can be further classified using recurrent genomic abnormalities including JAK1/STAT3 mutations, DUSP22 or TP63 translocations, loss of *TP53* and *PRDM1/BLIMP1*, and aberrant expression of ERBB4 [3, 4, 11]. However, the molecular mechanisms leading to ALK$^-$ALCL transformation, maintenance, and immune evasion remain quite elusive. Hyperactivation of STAT3 is documented in about 40–50% of ALK$^-$ ALCL [3], and contributes to the tumorigenesis and maintenance of STAT3+ ALCL via canonical gene regulation [3, 12] a paradigm shared by many human cancers. However, new findings suggest that STAT3 can also contribute to cancer tumorigenesis by regulating long noncoding RNA (lncRNA) [13, 14].

LncRNAs are transcripts, longer than 200 nucleotides, often display an intron–exon organization, and share close similarities to protein-coding genes. They have pleotropic properties, controlling gene expression, protein stability, localization and function, and cell identity [15]. Unbiased genome-wide analyses discovered thousands of lncRNAs, whose number outnumbers those of protein-coding RNAs. More than 8000 lncRNAs are aberrantly expressed in cancer, making these genes ideal tumor-specific biomarkers and putative targets for therapeutic interventions [16].

Remarkably, lncRNAs can shape the T-cell compartment and modulate the adaptive immune system [17]. Detectable lncRNAs are often located within the neighborhood of lineage-specific mRNA [17], and their dynamic expression is cell/stage-specific regulated [18] and linked to cell differentiation and identity [19]. Indeed, IFNG-AS1, lincCcr2–59AS, Th2 LCRR, and GATA3-AS1 are associated with distinct T-helper 1 (Th1) or Th2 phenotypes [20–22] while lincRNA-MAF-4 promotes T-lymphocyte differentiation by interacting with chromatin modifiers LSD1 and EZH2 via MAF [19]. Conversely, their oncogenic contributions in T-cell lymphoma remain poorly elucidated and their contribution to the ALCL phenotype remains unexplored [23–25].

Here, by performing deep expression profiling in conjunction with de novo transcriptome assembly, we discovered a panel of previously unknown lncRNAs of ALCL. We focused on a chromatin-associated lncRNA, selectively expressed by ALK$^-$ ALCL lymphoma, named *BlackMamba*. Mechanistically, *BlackMamba* is regulated via *STAT3* and its expression is required to sustain proliferation and clonogenicity of ALK$^-$ ALCL through the transcriptional regulation and the functional control of the lymphoid helicase HELLS. These findings provide new evidence on the mechanisms leading to STAT3-mediated ALCL transformation and foster the implementation of STAT3 target therapies for these lymphomas.

Materials and methods

Tissue samples

Fresh and viable cryopreserved cells were isolated from diagnostic/relapsed primary lymphoma biopsies. Diagnoses were assigned according to the WHO classification. Tissues used for NGS analyses were selected for their high tumor cell content (>50%). All studies were approved through institutional human ethics review boards, and patients provided written informed consent in accordance with the Declaration of Helsinki.

Cell growth, colony formation assays, and cell division

For cell growth assays, cells were washed with phosphate-buffered saline seeded at 2.5×10^5 cells/ml and treated with drugs. Viable cells were counted by trypan blue exclusion.

Colony formation assays were performed as previously described [26].

Cell division was evaluated using 5 µM of carboxyfluorescein succinimidyl ester (CFSE) fluorescent dye following the manufacturer's instructions (ab113853, Abcam). The fluorescence was read by FACSCanto II instrument after 6 or 9 days and data were analyzed using BD FACSDiva Software (BD).

Analysis of mRNA stability

Actinomycin D was used to inhibit nascent RNA synthesis. MAC2A, TLBR-1, and TLBR-2 cells (5×10^5 cells/ml)

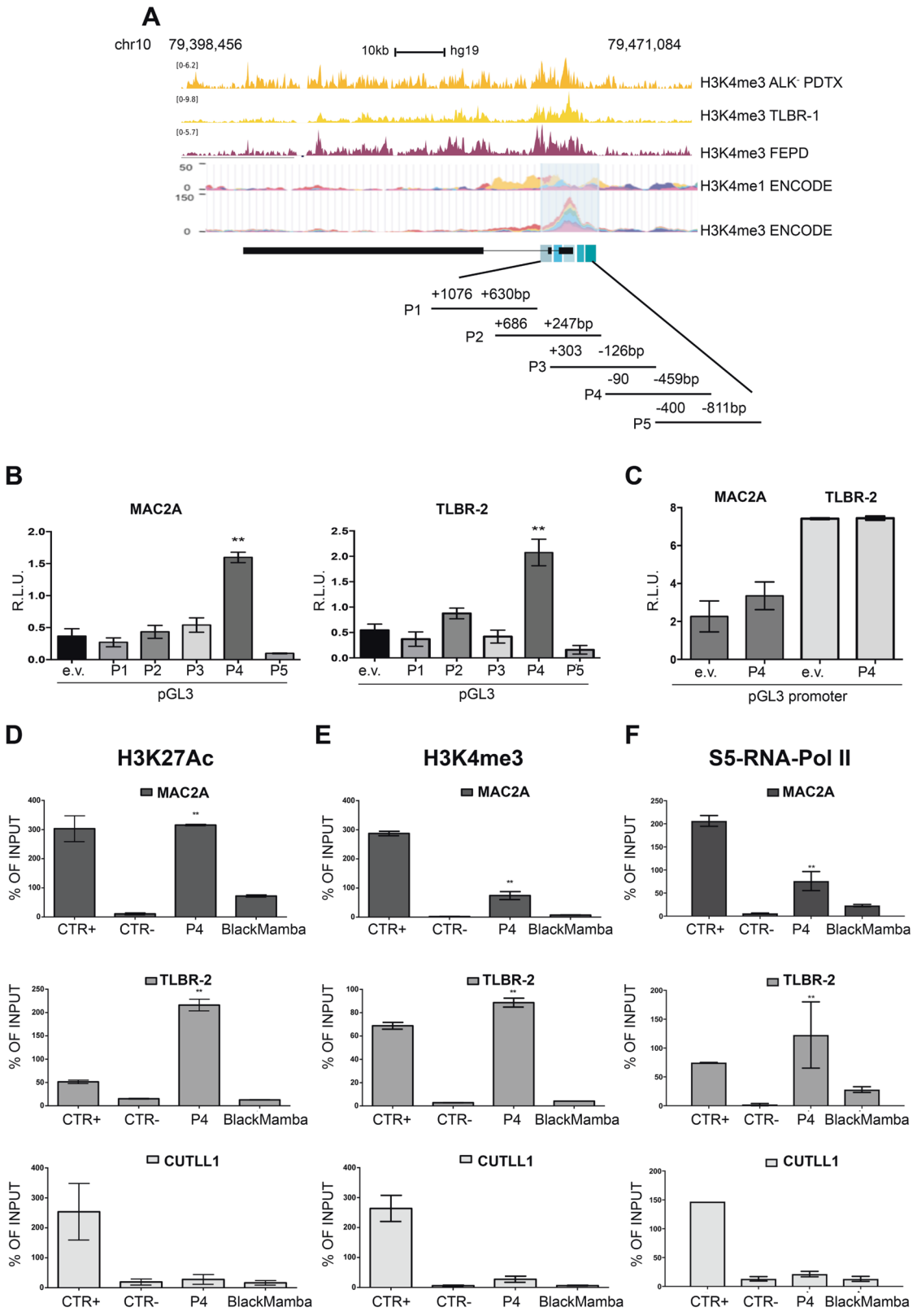
A
chr10 79,398,456
10kb hg19
79,471,084
H3K4me3 ALK- PDTX
H3K4me3 TLBR-1
H3K4me3 FEPD
H3K4me1 ENCODE
H3K4me3 ENCODE
P1 +1076 +630bp
P2 +686 +247bp
P3 +303 -126bp
P4 -90 -459bp
P5 -400 -811bp
B
MAC2A
TLBR-2
R.L.U.
e.v. P1 P2 P3 P4 P5
pGL3
C
MAC2A
TLBR-2
R.L.U.
e.v. P4 e.v. P4
pGL3 promoter
D
H3K27Ac
E
H3K4me3
F
S5-RNA-Pol II
% OF INPUT
CTR+ CTR- P4 BlackMamba
MAC2A
TLBR-2
CUTLL1

◀ **Fig. 2 *BlackMamba* is a previously unknown long noncoding RNA in ALK⁻ ALCL subset. a** Schematic representation of *BlackMamba* genomic locus showing the position and the level of histone modifications of the putative promoter and the representation of TSS region. Luciferase activity of overlapping fragments into pGL3 vector (**b**) and luciferase activity of P4 fragment into pGL3-promoter vector (**c**). Data are represented as normalized ratio of firefly-Renilla luciferase activities and are expressed as mean values ± SD ($n = 3$). $^{**}p \leq 0.01$. ChIP quantitative qRT-PCR detection of H3K27ac (**d**), H3K4me3 (**e**), and phospho- S5-RNA-polymerase II (**f**) on P4 fragment in a panel of cell lines. GAPDH promoter was used as CTR+ whereas, BlackMamba region +33,459 bp (*BlackMamba*) and a noncoding intergenic region (CTR−) served as negative controls. The values represent mean ± SEM ($n = 3$). $^{**}p \leq 0.01$.

were treated with actinomycin D or DMSO (5 µg/ml, Sigma-Aldrich) for 2, 4, 8, 16, and 24 h and collected for RNA isolation.

siRNA transfection

FEPD, MAC2A, TLBR-1, and TLBR-2 cells (1×10^6) were transfected with 5 or 10 pmoli siRNA using the Cell Line Nucleofector Kit SF and Amaxa 4D Nucleofector (program FI115 for FEPD and MAC2A, DS-130 for TLBR-2 and for TLBR-1). Twenty-four hours after transfection, cells were harvested and plated 2.5×10^5 cells/ml. For STAT3, we used a Silencer Select Validated siRNA ID:s743 (Ambion, Life Technologies); for *BlackMamba* we used three different Silencer Selected siRNAs (Ambion, Life Technologies) (Supplementary Table 1).

Luciferase assay

MAC2A and TLBR-2 cells (1×10^6) were transfected with 0.4 µg of reporter pGL3-luciferase plasmids using the Cell Line Nucleofector Kit SF and 4D Amaxa Nucleofector (program FI115 for MAC2A, DS-130 for TLBR-2).

Twenty-four hours after transfection, cells were harvested and luciferase activity was measured using the Dual-Luciferase Reporter Assay System (Promega) in a GloMax Discover Luminometer (Promega) according to the manufacturer's instructions. For each sample, firefly luciferase activity was normalized on *Renilla* luciferase activity and transactivation of the various reporter constructs was expressed as fold induction on empty vector (pGL3-basic or pGL3-promoter) activity.

Chromatin immunoprecipitation (ChIP)

ChIP experiments were performed as previously described [27]. Chromatin was precipitated with antibodies against H3K4me3 (Abcam-ab8580), H3K4me1 (Abcam-ab8895), H3K27Ac (Abcam-ab4729), RNA polymerase II STD repeat YSPTSPS ((phospho S5) (Abcam – ab5408), STAT3 (124H6 Mouse mAb#9139), HELLS (H-4, sc-46665 Santa Cruz), or IgG (as negative control). For each experiment, a chromatin amount corresponding to 0.5% of chromatin used for immunoprecipitation was kept as input control. Each qRT-PCR value was normalized over the appropriate input control and reported in graphs as % of input (qRT-PCR value/input value × 100).

RNA immunoprecipitation (RIP)

RIP was performed as described by Abcam RIP protocol. The precleared lysate was incubated for 2 h with 6 µg of antibodies specific for HELLS (sc-46665, Santa Cruz Biotechnology, Inc.) or with IgG as negative control. All experiments were repeated at least three times.

Quantitative PCR (qRT-PCR)

One microgram of total RNA was reverse transcribed using RT (iScript, Biorad). The amplified transcript level of each specific gene was normalized on CHMP2A housekeeping. ΔΔCt quantification method was used for RT-qPCR analyses.

The list of primers used is provided in Supplementary Table 2.

Western blot

Western blot analysis was performed using standard techniques [3]. The primary antibodies were: STAT3 (124H6 Mouse mAb#9139, 1:1000 Cell signaling Technology), pSTAT3 (Tyr705, D3A7 Rabbit mAb#9145, 1:1000 Cell signaling Technology), STAT5 (D2O6Y Rabbit mAb#94205, 1:1000 Cell signaling Technology) pSTAT5 (Tyr694, Rabbit mAb#9351, 1:1000 Cell signaling Technology), ALK (D5F3 Rabbit mAb#3633, 1:1000 Cell signaling Technology), pALK (Tyr1604, Rabbit mAb#3341, 1:1000 Cell signaling Technology), β-Actin (sc-47778, 1:1000 Santa Cruz Biotechnology, Inc.), and HELLS (sc-46665, 1:1000 Santa Cruz Biotechnology, Inc.). All secondary antibodies (rabbit and mouse) were HRP-conjugated (GE Healthcare) and diluted 1:5000.

Immunofluorescence

Immunofluorescences were performed as previously described [28].

Statistical analyses

Statistical analyses for identification and the analysis of lncRNAs are described in Supplementary methods.

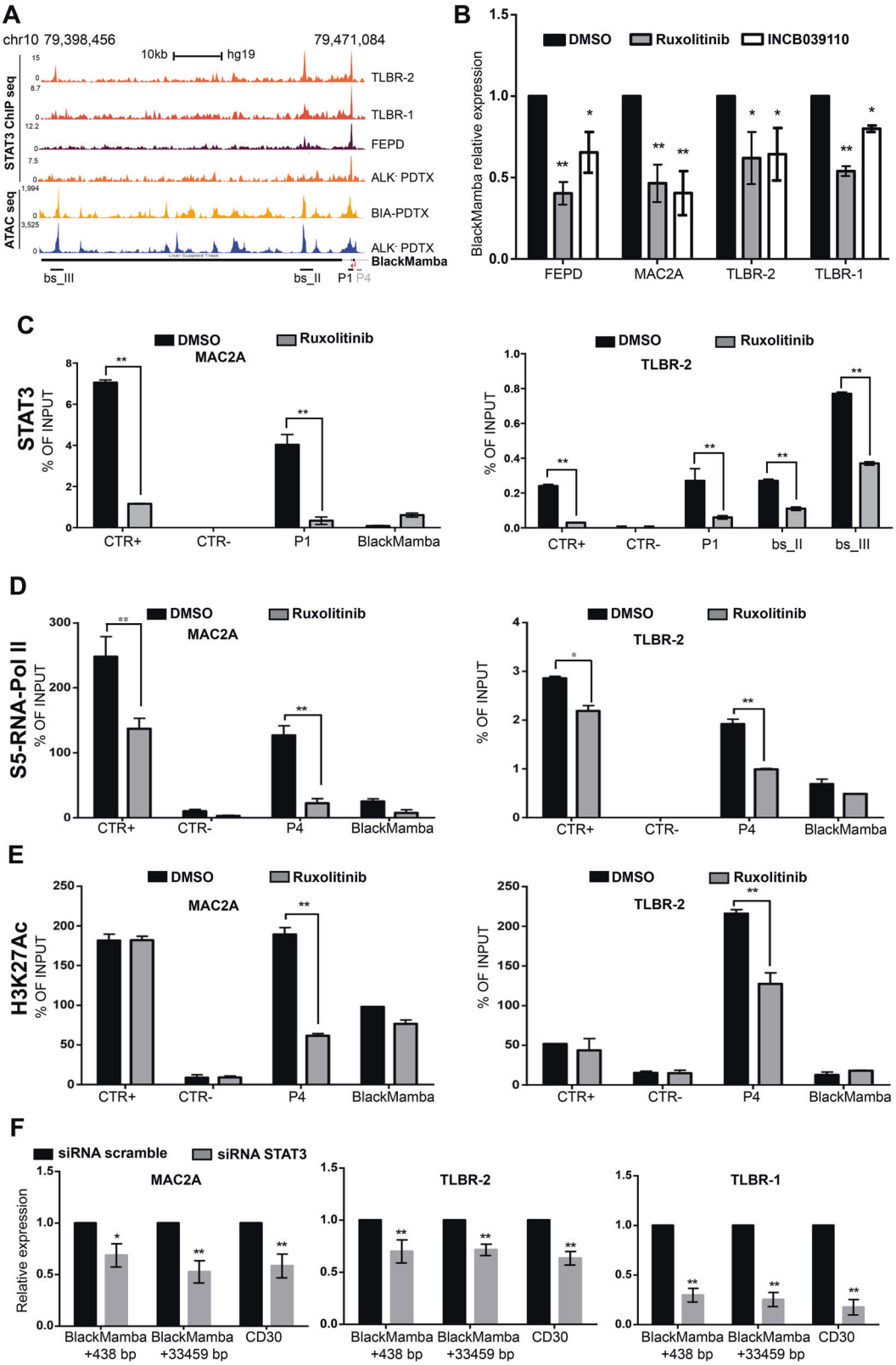
A
chr10 79,398,456
79,471,084
10kb
hg19
STAT3 ChIP seq
ATAC seq
TLBR-2
TLBR-1
FEPD
ALK- PDTX
BIA-PDTX
ALK- PDTX
BlackMamba
bs_III
bs_II
P1
P4
B
DMSO
Ruxolitinib
INCB039110
BlackMamba relative expression
FEPD
MAC2A
TLBR-2
TLBR-1
C
DMSO
Ruxolitinib
MAC2A
STAT3
% OF INPUT
CTR+
CTR-
P1
BlackMamba
TLBR-2
bs_II
bs_III
D
MAC2A
S5-RNA-Pol II
% OF INPUT
P4
TLBR-2
E
MAC2A
H3K27Ac
% OF INPUT
TLBR-2
F
siRNA scramble
siRNA STAT3
MAC2A
TLBR-2
TLBR-1
Relative expression
BlackMamba +438 bp
BlackMamba +33459 bp
CD30

◀ **Fig. 3 STAT3 regulates *BlackMamba* expression. a** STAT3 ChIP-sequencing analysis (top panel) and ATAC-sequencing analysis (bottom panel) along *BlackMamba* locus in ALK$^-$ ALCL cell lines and PDTX (Belli ALK$^-$ ALCL and IL89 BIA-ALCL). **b** qRT-PCR analysis of *BlackMamba* expression after 24 h of treatment with 1 μM of ruxolitinib or 2 μM of INCB039110. The values represent mean ± SD ($n = 3$) *$p \le 0.05$; **$p \le 0.01$. ChIP qRT-PCR detection of: (**c**) STAT3 antibody on P1 fragment, (**d**) Phospho-5 s RNA Polymerase II, and (**e**) anti-H3K27ac antibodies on P4 fragment of *BlackMamba* in ALK$^-$ ALCL cell lines treated for 24 h with 1 μM of ruxolitinib. BlackMamba region +33,459 bp *(BlackMamba)* was used as a negative control. ATF3 promoter was used as positive control for STAT3 binding, whereas GAPDH promoter was used as positive control for **d**, **e**. The values represent mean ± SEM ($n = 3$). **$p \le 0.01$; *$p \le 0.05$. **f** qRT-PCR analysis of *BlackMamba* in two different regions (+438 bp and +33,459 bp) in ALK$^-$ ALCL cells after transfection with specific STAT3-siRNA (96 hours). CD30 was used as positive control. The values represent mean ± SD ($n = 3$); *$p \le 0.05$; **$p \le 0.01$.

Statistical analyses were performed using GraphPad Prism Software (GraphPad). Statistical significance was determined using the Student's *t* test. Each experiment was replicated multiple time (>3 up to 6).

Results

ALCL express a large pool of previously unknown lncRNAs

To define lncRNAs preferentially associated with ALCL, we performed high coverage and directional RNA sequencing (RNA-Seq) of 21 ALK$^+$ ALCL and 16 ALK$^-$ ALCL primary samples. We included normal T-lymphocytes, corresponding to different stages of differentiation and 10 ALCL cell lines (Fig. 1a and Supplementary Table 3). Firstly, to confirm the appropriateness of pathological samples within our discovery set, we used a 3-gene model classifier (*TNFRSF8*, *BATF3*, *TMOD1)*, proven to accurately define ALK$^+$ and ALK$^-$ ALCL (Supplementary Fig. 1A) [6]. A principal component analysis based on canonical coding gene expression further resolved the discovery cohort into distinct clusters corresponding to normal T-cell and ALCLs (Supplementary Fig. 1B); the latter group was further stratified into two distinct subgroups, largely represented by ALK$^+$ and ALK$^-$ ALCL samples (Supplementary Fig. 1C).

Next, we executed a de novo transcriptome analysis of the aligned primary tumor samples [29], which identified 106,014 new transcripts. Applying filtering cutoffs based on transcript length, exon count, and coding potential (based on cross-species comparisons), we discovered 1208 previously unknown ALCL-specific lncRNAs (Fig. 1b). These lncRNAs showed transcript length >200 bp (a canonical lncRNAs feature), a stringent number of exons $n = 2$ for conserved spliced transcripts (Fig. 1c, d), and they displayed low coding potential compared to canonical coding RNAs (Fig. 1e).

Next, we identified a set of lncRNAs significantly overexpressed in ALCL samples (18/352) by unsupervised analysis (Supplementary Table 4). Even if this set was not able to fully discriminate ALK$^+$ and ALK$^-$ ALCL, these novel lncRNAs were found to be significantly overexpressed in ALCL compared with normal T-lymphocytes (Fig. 1f and Supplementary Fig. 1D, E). Then we restricted the analysis to lncRNAs expressed in at least 20% of ALCL samples (five or more samples), this analysis led to the discovery of a pool of 14 lncRNAs (FDR < 0.05) (Fig. 1g). Since the deregulated STAT3 signaling is oncogenic in ALCL [3, 12], we then searched for canonical STAT3 binding sites within putative promoter regions of these previously unknown lncRNAs (Fig. 1g). We identified the lncRNA XLOC_043524 only, which we named *BlackMamba*.

BlackMamba is a nonannotated lncRNA located on q26.3 of chromosome 10, predicted to be transcribed from the minus strand, with an estimated transcript length of 70,292 bp (Fig. 1) and with half-life of ~4 h (Supplementary Fig. 2a–d). *BlackMamba* is composed of three exons, lacking alternative isoforms. Within the discovery cohort, 9/16 ALK$^-$ ALCL (56%) and 1/21 ALK$^+$ ALCL (4.7%) expressed detectable levels of *BlackMamba*. The preferential expression of ALK$^-$ ALCL was further confirmed in an independent set of 15 ALCLs and 9 PTCLs, and no detectable transcripts were seen in a cross-validation cohort of healthy donor resting and activated PBMCs (Fig. 1i and Supplementary Table 5). When we extended this analysis to a panel of T-cell lines, we confirmed that *BlackMamba* expression was consistently detectable in ALK$^-$ ALCL and breast implanted associated (BIA)-ALCL cell lines, albeit with variable levels of expression, with TLBR-1 and TLBR-2 expressing the highest levels. Very low transcripts were detected in ALK$^+$ ALCL (L82 and Karpas299), systemic and cutaneous ALK-ALCL (FEPD, Mac1), and in cutaneous T-cell lymphoma MJ, while T-ALL lines (CUTLL1, KOPT-K1, and Jurkat), and mycosis fungoides HUTL-78 cells were negative (Fig. 1j).

BlackMamba is a promoter-associated lncRNA transcriptionally regulated by STAT3

To explore the mechanism(s) which regulates the expression of *BlackMamba*, we investigated the genomic elements responsible for its transcription. H3K4me3 profile by ChIP-seq in ALK$^-$ ALCL cell lines and patient-derived tumor xenograft (PDTX) (Belli) lines showed a high-density profile within a 2000 bp region, spanning the putative transcription start site (TSS) (Fig. 2a). These data are in agreement with a relatively high level of H3K4Me3 (but not

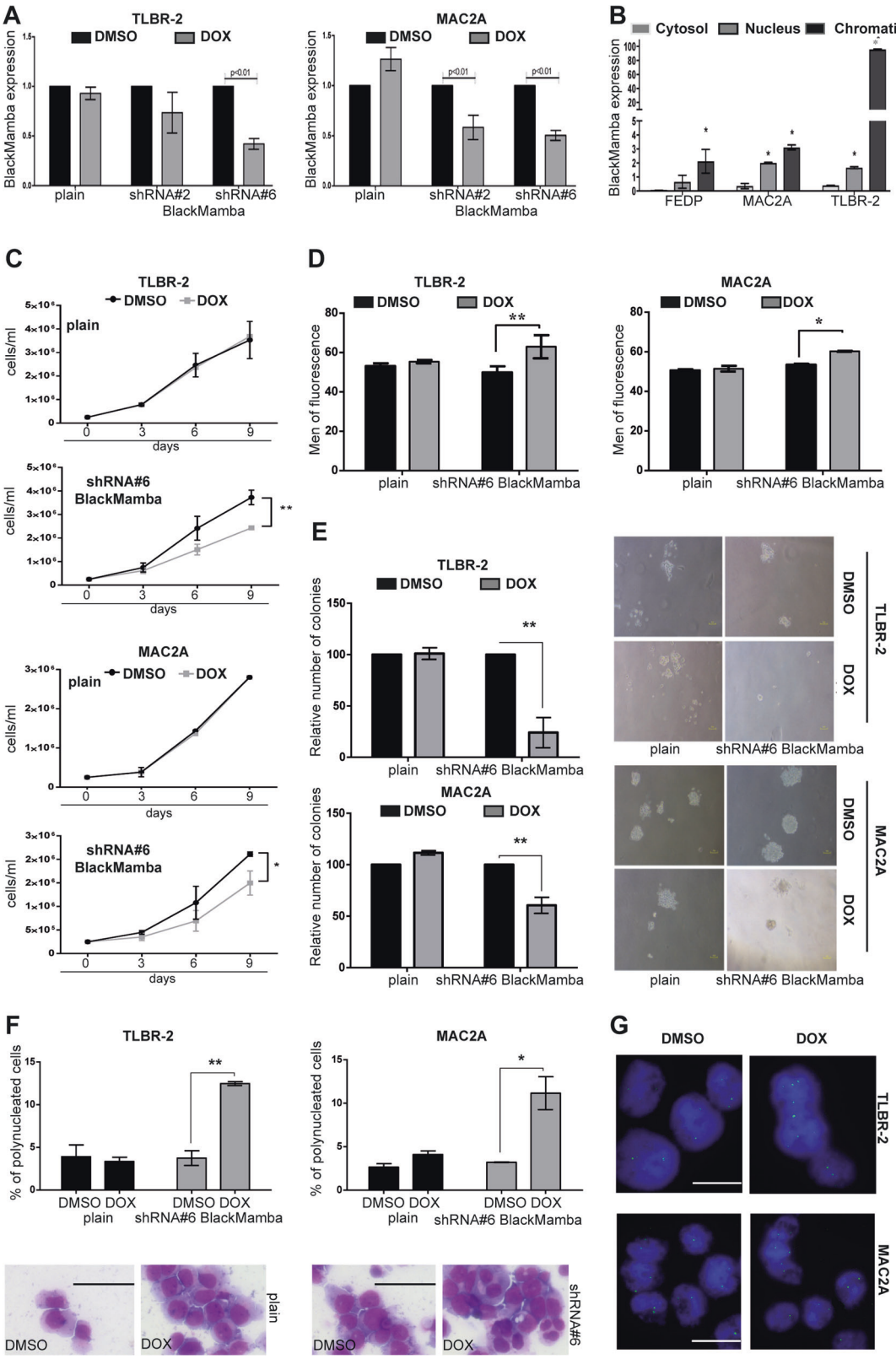

of H3K4Me1) within the same region in ENCODE (in several cell lines), suggesting that *BlackMamba* is likely to be a promoter-associated gene rather than an enhancer-associated RNA. To elucidate the promoter region of *BlackMamba*, we then cloned multiple DNA fragments upstream of a luciferase reporter cassette corresponding to a

◀ **Fig. 4 Loss of *BlackMamba* leads to impaired cell proliferation and clonogenicity of ALK⁻ ALCL cells. a** qRT-PCR analysis of *BlackMamba* expression after 6 days of doxycycline treatment in MAC2A and TLBR-2 cells. **b** Relative expression of *BlackMamba* in cytoplasm, nucleus, and chromatin fraction of ALK⁻ ALCL cell lines (average of three independent experiments ± S.D.) One-tailed *t*-test. $*p \le 0.05$. **c** Growth curve of MAC2A and TLBR-2 expressing pLKO-shRNA *BlackMamba* after induction with doxycycline. Each data point represents the mean ± S.D. ($n = 3$). One-tailed *t*-test. $*p \le 0.05$; $**p \le 0.01$. **d** The histograms show the fluorescent intensity of *CFSE*-labeled TLBR-2 and MAC2A expressing pLKO-shRNA *BlackMamba* (9 days of treatment). Each data point represents the mean ± S.D. ($n = 3$). One-tailed *t*-test. $*p \le 0.05$; $**p \le 0.01$. **e** Histogram shows methylcellulose colony formation of pLKO-shRNAs *BlackMamba* expressing cells pretreated with doxycycline for 6 days. Colonies were counted on day 10, after plating. Each data point represents the mean ± S.D. ($n = 3$). **f** The upper panel shows the percentage of polynucleated cells in at least 100 cells stained with May–Grunwald Giemsa (6 days after doxycycline induction). Each data point represents the mean ± S.D. ($n = 3$). $*p \le 0.05$; $**p \le 0.01$. The lower panel shows the polynucleated cells in TLBR-2. The scale bar represents 100 µm. **g** FISH analysis of chromosome 17 centromere in pLKO-shRNAs *BlackMamba* expressing TLBR-2 and MAC2A cells (6 days of doxycycline induction). The scale bar represents 10 µm.

region of 2000 bp (P1-P5), spanning from −811 to +1076 bp of the *BlackMamba* TSS (Fig. 2a). High luciferase signals were observed with the segment spanning from −459 bp to −90 bp (P4) in both MAC2A and TLBR-2 (Fig. 2b). By cloning P4 in an "enhancer-like" position downstream to the reporter gene, we demonstrated that this segment did not act as an enhancer (Fig. 2c). We next show that the H3K27Ac and H3K4Me3 marks were enriched in two ALK⁻ ALCL lines but not in *BlackMamba* negative CUTLL1 line (Fig. 2d, e). Likewise, the RNA-Pol II was found to be actively recruited on the P4 element only in the ALK⁻ ALCL cells (Fig. 2f).

ALK⁺ and ALK⁻ ALCLs can be addicted to JAK-STAT signaling pathway, and the loss of STAT3 signaling impairs their growth and survival [3, 12]. Because we initially predicted that *BlackMamba* had a canonical binding site for STAT3, we tested whether STAT3 could bind to the *BlackMamba* promoter. By STAT3 ChIP -Seq, ALK⁻ cell lines and PDTX displayed multiple STAT3 peaks in close proximity to the P1 or bs_II and bs_III sites of *BlackMamba* (Fig. 3a). These regions corresponded to accessible, active chromatin sites by ATAC-seq. (Fig. 3a). To test the *BlackMamba* dependence on the transcriptional activity of STAT3, we tested the level of STAT3 phosphorylation in a panel of cell lines (Supplementary Fig. 3A). Next, STAT3+ ALK⁻ ALCL cells were treated with a JAK1/2 (ruxolitinib) or a selective JAK1 inhibitor (INCB039110), demonstrating that after 24 h of treatment the mRNA expression of *BlackMamba* was downregulated (Fig. 3b). Consistent with ChIP-seq data, STAT3 was significantly enriched on identified regions of *BlackMamba* (Fig. 3c). Moreover, the JAKi treatment resulted in the specific inhibition of RNA-Pol II binding, reduced transcriptional activity and the concomitant modulation of H3K27Ac marks (Fig. 3d, e). Lastly, since the pharmacological inhibition of JAK/STAT can elicit a plethora of targets and trigger alternative events, we evaluated the expression of *BlackMamba* upon silencing of STAT3 by specific siRNA. Having first demonstrated that STAT3-siRNA could effectively reduce STAT3 expression (Supplementary Fig. 3B) and its canonical targets (i.e., CD30, Fig. 3f). we confirmed that the loss of STAT3 was associated with the downregulation of *BlackMamba* (Fig. 3f).

Remarkably, although the expression of BlackMamba was barely detectable in ALK⁺ALCL, the selective inhibition of ALK signaling (crizotinib) led to the downregulation of BlackMamba (Supplementary Fig. 3C).

Collectively, these data demonstrate that STAT3 regulates the expression of *BlackMamba*, independently from its upstream activators.

BlackMamba is required for active proliferation and clonogenicity of ALK⁻ ALCL cells

To test the biological properties of *BlackMamba*, we silenced its expression using two different approaches: a transient siRNA transfection and a doxycycline inducible shRNA. Because *BlackMamba* is a large gene (~70 kb), we targeted different regions (Supplementary Fig. 4A and Supplementary Table 2). We found two independent shRNAs that effectively reduced its expression after doxycycline induction in MAC2A (−50% for each shRNAs) without affecting top-scoring off-targets significantly (Supplementary Fig. 4B). Both shRNA#2 and #6 could effectively knockdown (KD) the lncRNA in TLBR-2, although with different potency (−30%, shRNA#2 and −60%, shRNA#6) (Fig. 4a). Next we studied the cellular localization of *BlackMamba* at steady state, demonstrating it was enriched in the nucleus and strongly associated to the chromatin fraction, suggesting a putative role in chromatin organization and gene expression regulation (Fig. 4b and Supplementary Fig. 4C).

Functionally, the KD of *BlackMamba* resulted in a dose-dependent cell growth inhibition (Fig. 4c and Supplementary Fig. 4D, E), in the absence of an increased rate of apoptosis (Supplementary Fig. 4F). This phenotype was reproducibly detected in shRNA#6-treated ALCL cells, although significant shRNA#2 mediated changes were observed only in MAC2A cells, which expressed lower levels of mRNA (Supplementary Fig. 4G). Next we demonstrated a delayed cell division in *BlackMamba* KD cells (Fig. 4d and Supplementary Fig. 4H, I), and an impaired ALCL lymphoma colony formation (Fig. 4e). Conversely, the growth and survival in control K562 (chronic myeloid leukemia) and CUTLL1 KD cell lines

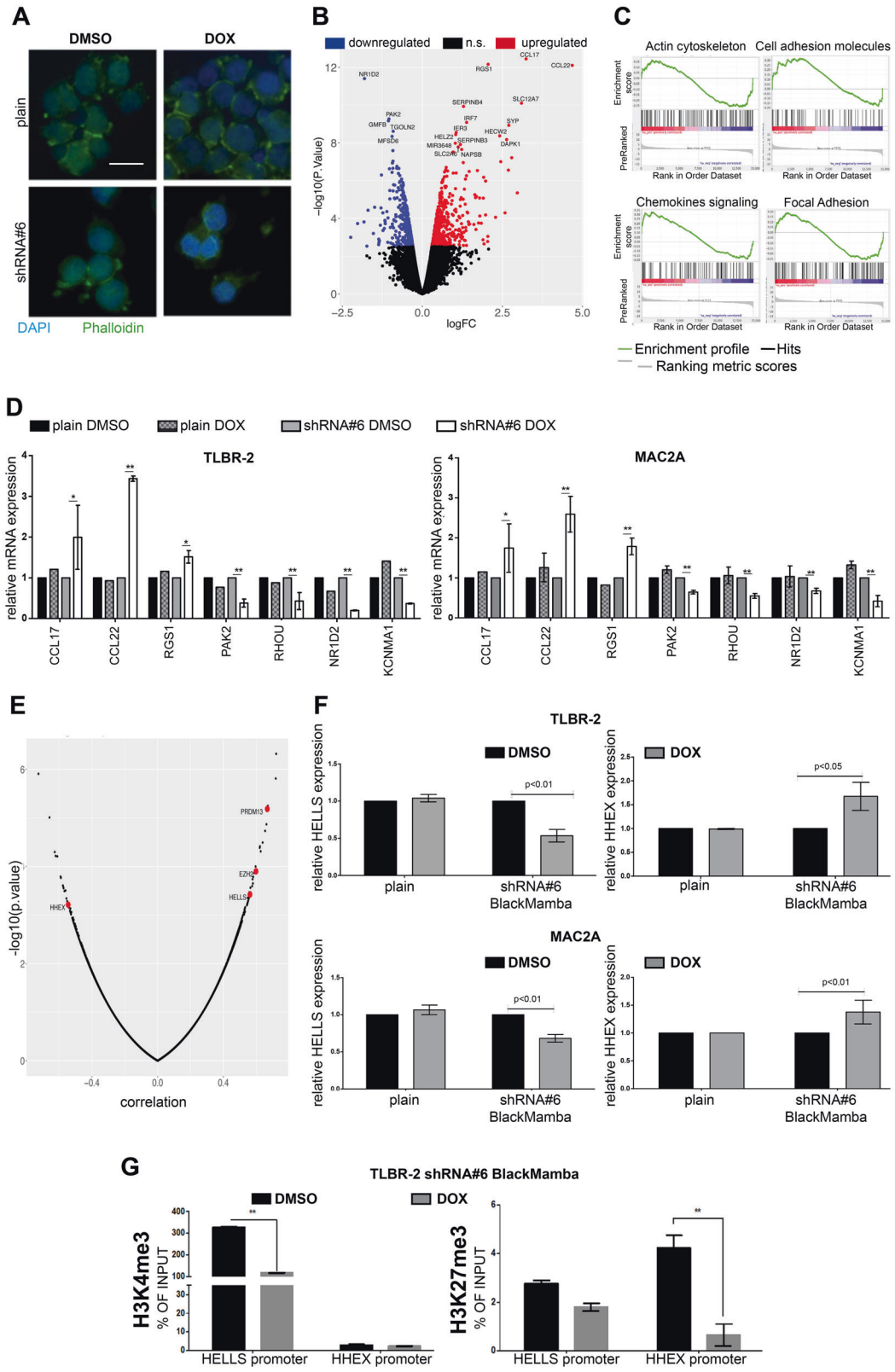

were not affected (Supplementary Fig. 4J). Interestingly, the cytological inspection of May–Grunwald Giemsa stained ALK⁻ALCL cells upon *BlackMamba* KD showed an increased number of polynucleated cells (Fig. 4f and Supplementary Fig. 4K), with a polyploid DNA content by partial FISH-based karyotyping (Fig. 4g).

◀ **Fig. 5 BlackMamba regulates the lymphoid-specific helicase HELLS. a** Immunofluorescence images of TLBR-2 expressing pLKO-shRNA#6 *BlackMamba* stained with antiphalloidin antibody after doxycycline treatment (6 days). The scale bar represents 10 µm. **b** Volcano plot analysis of TLBR-2 expressing pLKO-shRNAs#6 *BlackMamba* after 6 days of doxycycline induction. **c** GSEA analyses of downregulated and upregulated pathways in TLBR-2 expressing pLKO-shRNA#6 *BlackMamba*. **d** qRT-PCR analysis of a panel of genes in MAC2a and TLBR-2 expressing pLKO-shRNA#6 *BlackMamba* after 6 days of doxycycline induction. **e** Graph shows the expression correlation between *BlackMamba* and protein-coding genes in ALK$^-$ ALCL samples. PRDM13, HELLS, and EZH2 showed significant positive co-regulation while HHEX showed a negative co-regulation. **f** qRT-PCR analysis of HELLS (6 days after doxycycline induction) and HHEX (9 days after doxycycline induction) expression in ALK$^-$ ALCL cell lines. Each data point represents the mean ± S.D. ($n = 3$). One-tailed *t*-test. $^*p \le 0.05$; $^{**}p \le 0.01$. **g** ChIP qRT-PCR detection of H3K4me3 and H3K27me3 antibodies on HELLS and HHEX promoters in TLBR-2 expressing pLKO-shRNA#6 *BlackMamba* (6 days after doxycycline induction). The experiment was representative of a triplicate. The bars represent the mean ± SEM ($n = 3$). $^{**}p \le 0.01$.

Lastly, since cytokinesis requires an appropriate cytoskeleton organization, we investigated the cytoskeleton architecture of *BlackMamba* silenced cells. As actin filaments are major components of the contractile structure that guide cytokinesis in eukaryotes [30], we examined the cellular cytoskeleton using phalloidin staining of actin filaments. We found that after *BlackMamba* KD, cells lose actin polarization and have a displacement of filaments from their membrane localization, supporting its role in cytoskeleton reorganization and cytokinesis (Fig. 5a). This hypothesis is supported by the transcriptional changes observed after RNA sequencing in *BlackMamba* KD (59 downregulated genes and 61 significantly upregulated genes, ≥2-fold and FDR < 0.05, Fig. 5b and Supplementary Table 6) where top-scored genes modulated (i.e., RGS1, CCL22, CCL17, PAK2, RHOU) epitomize by the modulation of actin cytoskeleton, integrin-mediated cell adhesion, and focal adhesion genes (Fig. 5c, d and Supplementary Fig. 5A)

Overall these data suggest that *BlackMamba* is involved in the maintenance of appropriate completion of cytokinesis.

BlackMamba regulates the transcription of the lymphoid-specific DNA helicase HELLS

Chromatin-enriched lncRNAs are spatially correlated with transcription factors [31], can act as cell type-specific activators of proximal gene transcription [32] and chromatin-associated lncRNAs (such as XIST or KCNQ1ot1) can influence local chromatin organization, leading to in *cis* transcriptional repression of genes within large genomic regions [33].

To test whether *BlackMamba* could operate according to this model, we correlated its expression with transcriptional factors and chromatin-remodeling genes (16 ALK$^-$ ALCL and 21 ALK$^+$ ALCL samples). The lymphoid-specific helicase (LSH) HELLS, the SET domain containing protein PRDM13, and the polycomb repressive complex 2 histone-lysine N-methyltransferase EZH2 were found to be positively correlated with *BlackMamba*. Conversely, the homeobox protein HHEX showed a negative correlation (Fig. 5e). To test whether this association was directly linked to *BlackMamba* expression, we quantified the mRNA levels of HELLS and HHEX in inducible shRNA *BlackMamba* ALCL cells. HELLS expression was consistently downregulated upon *BlackMamba* silencing, while HHEX was upregulated (Fig. 5f and Supplementary Fig. 5B). No consistent changes were observed for EZH2 (Supplementary Fig. 5C) while PRDM13 mRNA was undetectable (data not shown). In line with the gene expression changes, H3K4me3 and H3K27me3 underwent chromatin reorganization, with a significant reduction of H3K4me3 binding on HELLS promoter and a parallel loss of H3K27Me3 on HHEX promoter after silencing (Fig. 5g).

Being also HHEX and HELLS the only TFs located on the same chromosome of *BlackMamba*, we hypothesed that *BlackMamba* could regulate gene expression in *cis*.

To enforce this concept, we quantified the mRNA levels of several neighboring genes spanning 1 Mb from BlackMamba locus. After BlackMamba KD, 5/6 genes were concordantly downregulated in MAC2A and TLBR-2 cell lines (Supplementary Fig. 5D).

These data support the model which predicts that *BlackMamba* regulates in *cis* the expression of genes located on the same chromosome.

BlackMamba interacts with HELLS to control the *BlackMamba*-dependent transcriptional program

HELLS, also known as LSH or proliferation-associated SNF2-like (PASG), belongs to a large family of SNF2 chromatin-remodeling ATPases. HELLS is critical to the normal development and survival of lymphoid cells [34] and regulates chromatin organization and gene expression [35, 36]. HELLS mutations or misregulated expression were seen in several cancers and some cases of ICF syndrome [37].

To test whether HELLS enforces *BlackMamba*-mediated transcription, we silenced HELLS by specific shRNAs. qRT-PCR and WB analyses confirmed an effective silencing (Fig. 6a, b and Supplementary Fig. 6A), demonstrating the concomitant downregulation of known target BMI-1 and MLL1 genes [38, 39] (Supplementary Fig. 6B). Interestingly, the loss of HELLS was linked to expression changes of RGS1, CCL17, CCL22, PAK2, and KCNMA1, phenocoping the *BlackMamba* KD phenotype (Fig. 6c).

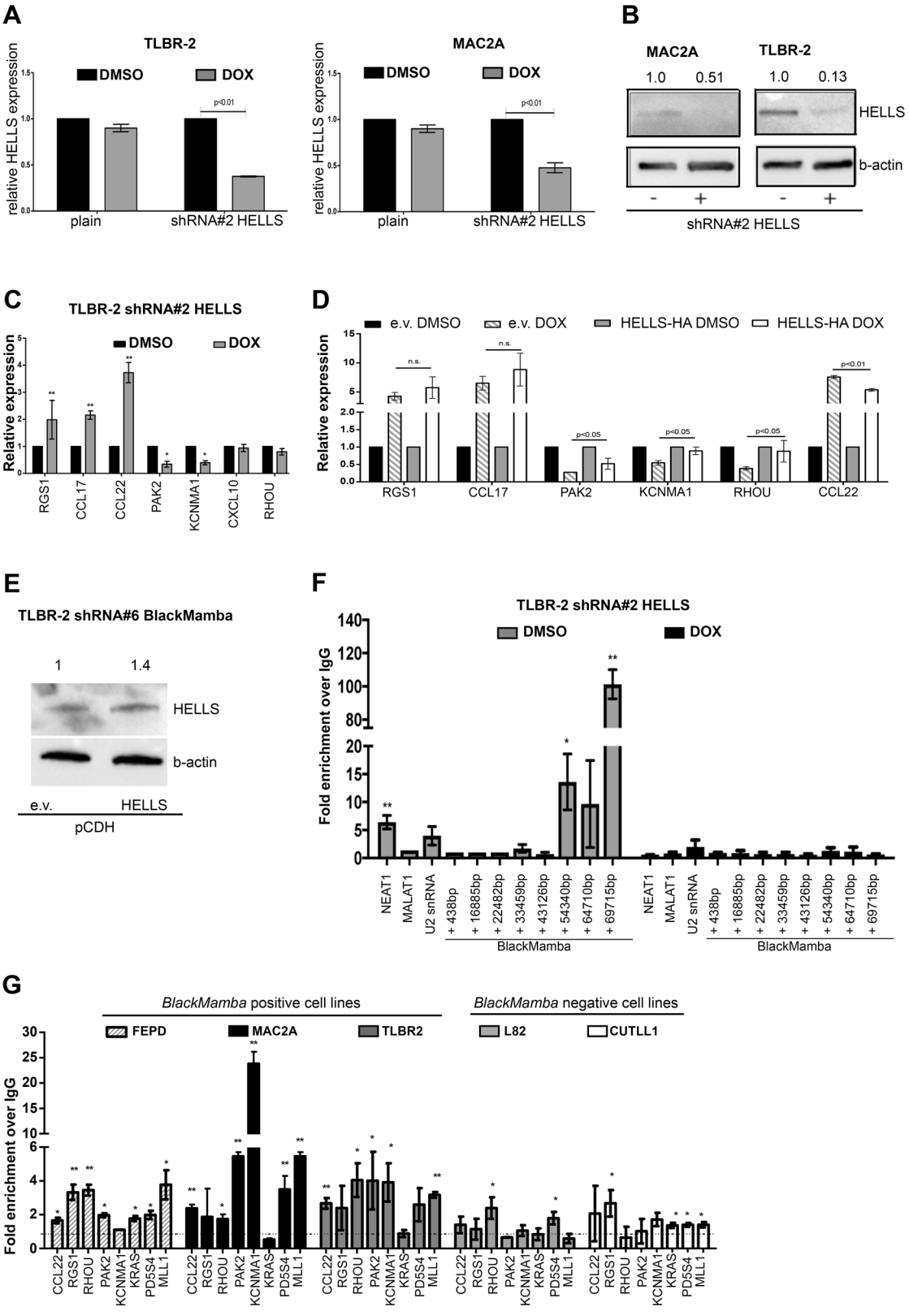

Conversely, the ectopic expression of HELLS effectively restored the baseline expression of these genes in *BlackMamba* KD cells (Fig. 6d, e).

It is known that lncRNAs control gene expression by recruiting chromatin-remodeling complexes to target promoters or enhancers, thereby influencing histone

◀ **Fig. 6 *BlackMamba* controls the recruitment of HELLS on multiple target promoters. a** qRT-PCR analysis of HELLS in ALK$^-$ ALCL cell lines expressing pLKO-shRNA#2 against HELLS (48 h after doxycycline induction). **b** Western blot shows the reduction of HELLS in cells expressing pLKO-shRNA#2 HELLS after 3 days of doxycycline induction. **c** qRT-PCR analysis of a panel of genes after 2 days of doxycycline induction in TLBR-2 expressing pLKO-shRNA#2 HELLS. Each data point represents the mean ± SEM. ($n = 3$). *$p \le 0.05$; **$p \le 0.01$. **d** qRT-PCR analysis of TLBR-2 cells co-expressing shRNA#6 *BlackMamba* and pCDH-HELLS-HA vectors (6 days after doxycycline induction). **e** Western blot shows the over-expression of ectopic HELLS-HA in TLBR-2 overexpressing pLKO-shRNA#6 *BlackMamba*. **f** RIP assay for HELLS in TLBR-2 expressing pLKO-shRNA#2 HELLS (2 days). Fold enrichment is relative to IgG (average of six independent experiments ±SEM; *$p \le 0.05$; **$p \le 0.01$). **g** ChIP qRT-PCR detection of HELLS antibody on several *BlackMamba* target gene promoters in a panel of T-cell lymphoma lines. MLL1, PD5S4 were used as positive controls (average of six independent experiments ±SEM; *$p \le 0.05$; **$p \le 0.01$).

modifications and chromatin accessibility [40]. Since the chromatin-remodeling properties of HELLS can be mediated by the lncRNA HOTAIR [41], we reasoned that *BlackMamba* might interact with HELLS to mediate its recruitment to target genes. To prove a direct association between HELLS and *BlackMamba*, we used RNA immunoprecipitation [3] and showed that HELLS binds to two distinct regions of BlackMamba at the 3′-end of the lncRNA (Fig. 6f). No readout was seen in HELLS KD cells. Next, we proved that HELLS was preferentially bound to target gene promoters only in *BlackMamba*-positive ALK$^-$ ALCLs independently from HELLS basal expression level (Fig. 6g and Supplementary Fig. 6C).

Collectively, these data demonstrate that BlackMamba-HELLS could be a part of the regulatory complex that occupied loci to coordinate ALK$^-$ ALCL transcriptional program.

HELLS is required for the maintenance of the neoplastic phenotype of ALK$^-$ ALCL

To determine the contribution of HELLS and *BlackMamba* in the maintenance of ALCL phenotype, we first investigated the cell growth capacity of HELLS KD cells. Indeed, the loss of HELLS led to an impaired cell growth (Fig. 7a and Supplementary Fig. 6D), reduced duplication rate (Fig. 7b), and clonogenicity (Fig. 7c and Supplementary Fig. 6E), a phenotype associated with an increased number of polynucleated cells, phenocopying the *BlackMamba* KD cells (Fig. 7d and Supplementary Fig. 6F).

Next we proved that the overexpression of HELLS could counteract the phenotype associated with the KD of *BlackMamba*, as the growth impairment of TLBR-2 cells expressing inducible shRNA against *BlackMamba* was effectively rescued (Fig. 7e) a finding associated with the mitigation of the polynucleated phenotype of the BlackMamba KD (Fig. 7f).

Overall, these findings demonstrate that HELLS is an essential downstream mediator of *BlackMamba* and that *BlackMamba*-HELLS axis represents a vulnerability of ALCL cells.

Discussion

Although a more complete genomic annotation of ALK$^-$ ALCL is emerging [42, 43], the mechanistic modalities of action remain elusive even for known recurrent defects [4, 42].

Here we describe a new chromatin-associated lncRNA, named *BlackMamba*, preferentially expressed in ALK$^-$ ALCL. Mechanistically, STAT3 regulates the expression of *BlackMamba* and its expression is required for ALK$^-$ ALCL neoplastic phenotype. This is achieved mainly through the action of the LSH, HELLS (Fig. 7g) and the transcriptional regulation of genes controlling G-protein and cytoskeletal organization, cell migration, tissue recruitment, and inflammation.

While emerging evidence have shown that lncRNAs are pathogenetic in human B-cell hematological neoplasms [44], little is known in mature T-cell neoplasms [23–25, 45]. In this study, we identified 1208 previously unknown lncRNAs linked to normal or neoplastic T-cells and among them, 18 lncRNAs were largely restricted to ALCL. Accordingly, a third of these new lncRNAs were co-shared by both ALCL subtypes, supporting the notion that both ALK$^+$ and ALK$^-$ ALCL can share some communalities [46].

Deregulated activation of STAT3 is a hallmark of many human cancers [47]. ALK$^+$ ALCL and a subset of ALK$^-$ ALCL have been proven to be addicted to the JAK/STAT signaling pathway [3, 48] and BIA-ALCL display a constitutive JAK/STAT deregulation [49]. Here, BIA-ALCL cell lines, as well as PDTX, were found to express high levels of *BlackMamba*. In ALCL, the deregulation/activation of JAK/STAT pathway is mediated by gene fusions, somatic mutations [50], and loss of negative regulators [7, 51]. These lead to a distinct transcriptional program associated with defined pathological entities [6, 46]. LncRNAs have been also shown to be linked to STAT signaling by modulating metabolic pathways [52] and conversely, STAT3, controlling the expression of lncRNAs, can regulate cell differentiation [17].

BlackMamba is a target of STAT3. Both siRNA-mediated and pharmacological inhibitions of JAK/STAT3 pathway profoundly repressed *BlackMamba* expression demonstrating its contribution in cell growth and clonal expansion of ALCL. Interestingly, loss of the *BlackMamba*

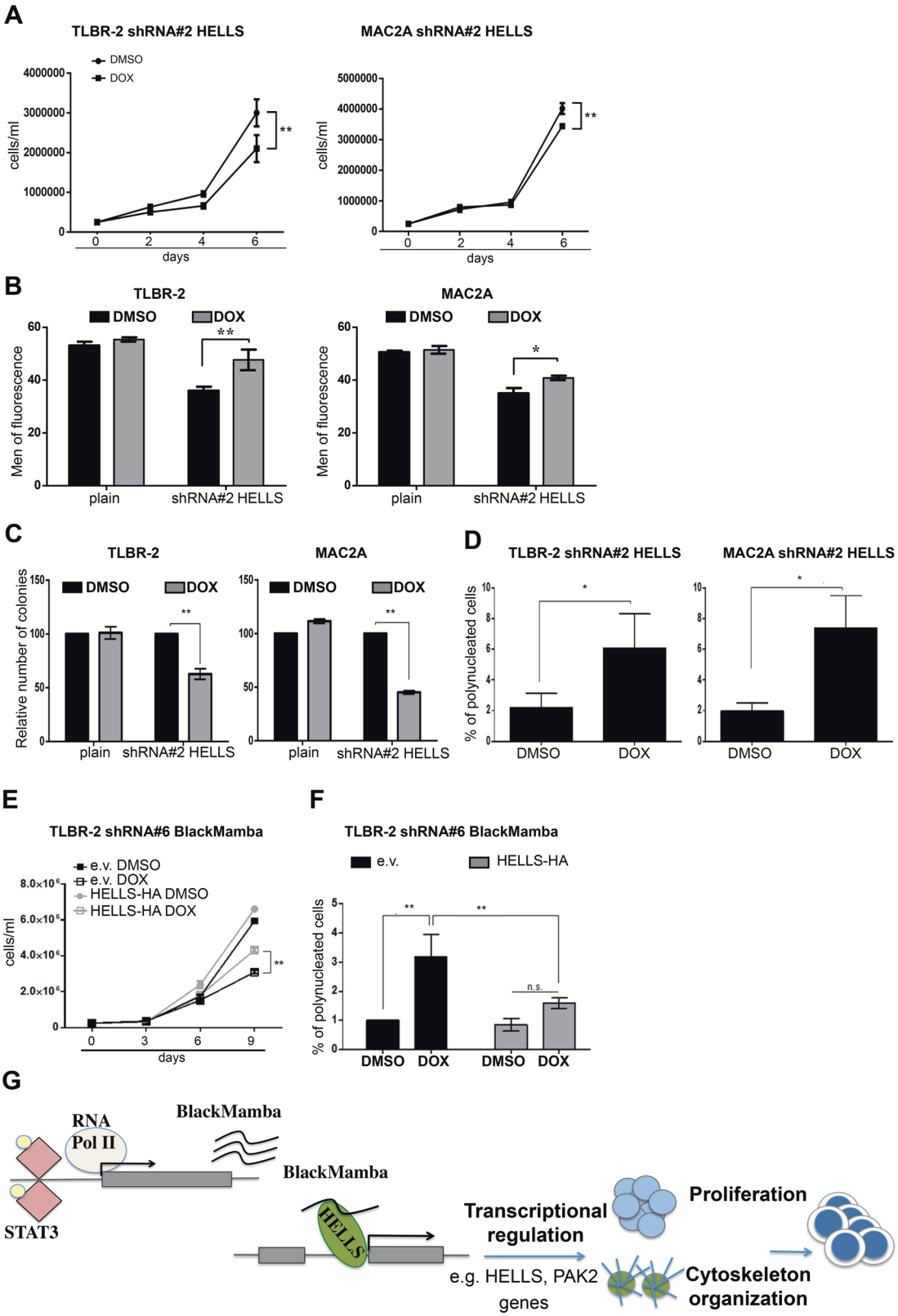

expression was linked to a unique phenotype characterized by an increased number of polynucleated cells with a balanced chromosomal enumeration possibly linked to key genes regulating cytoskeleton and cell motility. As STAT3 can regulate cell migration via RAC1 and Rho [53, 54], our data provide a new layer of complexity demonstrating a

◀ **Fig. 7 Silencing of HELLS mimics *BlackMamba* silencing phenotype. a** Growth curve of cells expressing pLKO-shRNA#2 HELLS. Each data point represents the mean ± S.D. ($n = 3$). ** $p \le 0.01$. **b** The histograms show the fluorescent intensity of *CFSE*-labeled ALK$^-$ ALCL cells (6 days after doxycycline treatment). **c** Histograms show methylcellulose colony formation of 3 days doxycycline pretreated cells expressing pLKO-shRNA#2 HELLS. Colonies were counted on day 10, after plating. Each data point represents the mean ± S.D. ($n = 3$). ** $p \le 0.01$. **d** Histograms show the percentage of polynucleated cells in at least 100 cells stained with May–Grunwald Giemsa (2 days of doxycycline induction). Each data point represents the mean ± S.D. ($n = 3$). * $p \le 0.05$. **e** Growth curve of TLBR-2 cells co-expressing pLKO-shRNA#6 *BlackMamba* and pCDH-HELLS-HA. Each data point represents the mean ± S.D. ($n = 3$). ** $p \le 0.01$. **f** The panel shows the percentage of polynucleated cells in at least 100 cells stained with May–Grunwald Giemsa (2 days of treatment). Each data point represents the mean ± S.D. ($n = 3$). ** $p < 0.01$. **g** Graphical model of putative tumorigenic role BlackMamba in ALK$^-$ALCL.

new role for STAT3 in cell shape and cytoplasmic partition via the axis of *BlackMamba*-HELLS. This model is supported by phenotype seen in HELLS KD cells, arguing that HELLS represents a critical downstream effector of *BlackMamba*.

Mechanistically, *BlackMamba* also contributes to the neoplastic phenotype of ALCL via multiple mediators, modulating a large group of genes encoding chemokines and chemokine receptors (CCL17–22 and CXCL10), G-protein regulators (RGS1) and multiple proteins involved in cell growth and motility (PAK2, ERBB2, RHOU, KIF21b).

Among *BlackMamba* targets, we found HELLS (16,550,000 bp from the locus of *BlackMamba*). HELLS controls T-cell growth [34], regulates DNA methylation [55], and modulates the epigenetic states at specific enhancers of key cell cycle regulators [56]. In cancer cells, HELLS sustains glioma stemness and through the interaction with E2F3 controls cell proliferation of prostate cancer cells [38, 57]. By interacting with the epigenetic silencer factor G9a, HELLS represses gene transcription [58]. Remarkably, a recent genome-scale CRISPR-Cas9 screen has shown cancer dependencies to DNA helicase and identified ATP-DNA helicases as promising new synthetic lethal targets in tumors [59]. Our work extends these findings providing a new lncRNA-dependent mechanism controlling the recruitment of HELLS on chromatin sites and its expression in lymphomas.

Our data provide novel insights into the transformation of ALCL via the untapped role of a lncRNA. Collectively, the findings further support the design of target therapeutic strategies to pharmacologically ablate/inhibit the expression of STAT3 and encourages novel discovery programs for the selection of compounds which could impair STAT3-downstream effector elements like HELLS. Lastly, since HELLS is expressed in many human tumors and plays a relevant role in DNA repair and genomic stability of cancers, its pharmacological inhibition represents a viable therapeutic strategy in many human cancers.

Data availability

BlackMamba sequence has been deposited in GenBank database with the accession number MN902222.

Acknowledgements We thank Dr Alan Epstein, who provided the TLBR-1 and 2 cells lines. We also thank Marina Grassi for technical help and Jacqueline Costa for English editing. This work was funded by the Italian Association for Cancer Research Special Program in Clinical Molecular Oncology, Milan (5 × 1000 No. 10007, GI), 7011-16 SCOR grant from the Leukemia & Lymphoma Society/SCOR grant (GI), by the Ministero della Salute (Ricerca Finalizzata No. GR-2016-02364298, VF), and R35GM122515 (JS). We thank the Epigenetic Core at Weill Cornell Medicine and the Genome Technology Center at New York University and GRADE Onlus Foundation.

Author contributions All authors contributed as a team to the experimental design and the interpretation of data. VF, AT, GM, and VM performed experiments and data analysis. AV and RB performed bioinformatics analysis. OE supervised bioinformatics analysis. EZ performed FISH staining. GI, JI, TBH, FM, and VF diagnosed and stratified pathological samples. RW and DF performed the sequencing. VF and GI created the pathological and clinical database. PL, WC, and JK contributed to the data analyses. GI, VF, and AC wrote the manuscript.

Compliance with ethical standards

Conflict of interest The authors declare that they have no conflict of interest.

Publisher's note Springer Nature remains neutral with regard to jurisdictional claims in published maps and institutional affiliations.

References

1. Swerdlow SH, Campo E, Pileri SA, Harris NL, Stein H, Siebert R, et al. The 2016 revision of the World Health Organization classification of lymphoid neoplasms. Blood. 2016;127:2375–90.
2. Hapgood G, Savage KJ. The biology and management of systemic anaplastic large cell lymphoma. Blood. 2015;126:17–25.
3. Crescenzo R, Abate F, Lasorsa E, Tabbo F, Gaudiano M, Chiesa N, et al. Convergent mutations and kinase fusions lead to oncogenic STAT3 activation in anaplastic large cell lymphoma. Cancer Cell. 2015;27:516–32.
4. Parrilla Castellar ER, Jaffe ES, Said JW, Swerdlow SH, Ketterling RP, Knudson RA, et al. ALK-negative anaplastic large cell lymphoma is a genetically heterogeneous disease with widely disparate clinical outcomes. Blood. 2014;124:1473–80.
5. Ferreri AJ, Govi S, Pileri SA, Savage KJ. Anaplastic large cell lymphoma, ALK-negative. Crit Rev Oncol Hematol. 2013;85:206–15.
6. Agnelli L, Mereu E, Pellegrino E, Limongi T, Kwee I, Bergaggio E, et al. Identification of a 3-gene model as a powerful diagnostic tool for the recognition of ALK-negative anaplastic large-cell lymphoma. Blood. 2012;120:1274–81.
7. Pizzi M, Gaudiano M, Todaro M, Inghirami G. Anaplastic lymphoma kinase: activating mechanisms and signaling pathways. Front Biosci. 2015;7:283–305.

8. Savage KJ, Harris NL, Vose JM, Ullrich F, Jaffe ES, Connors JM, et al. ALK- anaplastic large-cell lymphoma is clinically and immunophenotypically different from both ALK+ ALCL and peripheral T-cell lymphoma, not otherwise specified: report from the International Peripheral T-Cell Lymphoma Project. Blood. 2008;111:5496–504.
9. Boi M, Rinaldi A, Kwee I, Bonetti P, Todaro M, Tabbo F, et al. PRDM1/BLIMP1 is commonly inactivated in anaplastic large T-cell lymphoma. Blood. 2013;122:2683–93.
10. Iqbal J, Wright G, Wang C, Rosenwald A, Gascoyne RD, Weisenburger DD, et al. Gene expression signatures delineate biological and prognostic subgroups in peripheral T-cell lymphoma. Blood. 2014;123:2915–23.
11. Scarfo I, Pellegrino E, Mereu E, Kwee I, Agnelli L, Bergaggio E, et al. Identification of a new subclass of ALK-negative ALCL expressing aberrant levels of ERBB4 transcripts. Blood. 2016;127:221–32.
12. Chiarle R, Simmons WJ, Cai H, Dhall G, Zamo A, Raz R, et al. Stat3 is required for ALK-mediated lymphomagenesis and provides a possible therapeutic target. Nat Med. 2005;11:623–9.
13. Wang H, Huo X, Yang XR, He J, Cheng L, Wang N, et al. STAT3-mediated upregulation of lncRNA HOXD-AS1 as a ceRNA facilitates liver cancer metastasis by regulating SOX4. Mol Cancer. 2017;16:136.
14. Zhao J, Du P, Cui P, Qin Y, Hu C, Wu J, et al. LncRNA PVT1 promotes angiogenesis via activating the STAT3/VEGFA axis in gastric cancer. Oncogene. 2018;37:4094–109.
15. Kopp F, Mendell JT. Functional classification and experimental dissection of long noncoding RNAs. Cell. 2018 ;172:393–407.
16. Schmitt AM, Chang HY. Long noncoding RNAs in cancer pathways. Cancer Cell. 2016;29:452–63.
17. Aune TM, Crooke PS,III, Spurlock CF 3rd. Long noncoding RNAs in T lymphocytes. J Leukoc Biol. 2016;99:31–44.
18. Casero D, Sandoval S, Seet CS, Scholes J, Zhu Y, Ha VL, et al. Long non-coding RNA profiling of human lymphoid progenitor cells reveals transcriptional divergence of B cell and T cell lineages. Nat Immunol. 2015;16:1282–91.
19. Ranzani V, Rossetti G, Panzeri I, Arrigoni A, Bonnal RJ, Curti S, et al. The long intergenic noncoding RNA landscape of human lymphocytes highlights the regulation of T cell differentiation by linc-MAF-4. Nat Immunol. 2015;16:318–25.
20. Collier SP, Henderson MA, Tossberg JT, Aune TM. Regulation of the Th1 genomic locus from Ifng through Tmevpg1 by T-bet. J Immunol. 2014;193:3959–65.
21. Spurlock CF III, Tossberg JT, Guo Y, Collier SP, Crooke PS III, Aune TM. Expression and functions of long noncoding RNAs during human T helper cell differentiation. Nat Commun. 2015;6:6932.
22. Koh BH, Hwang SS, Kim JY, Lee W, Kang MJ, Lee CG, et al. Th2 LCR is essential for regulation of Th2 cytokine genes and for pathogenesis of allergic asthma. Proc Natl Acad Sci USA. 2010;107:10614–9.
23. Baytak E, Gong Q, Akman B, Yuan H, Chan WC, Kucuk C. Whole transcriptome analysis reveals dysregulated oncogenic lncRNAs in natural killer/T-cell lymphoma and establishes MIR155HG as a target of PRDM1. Tumour Biol. 2017;39:1010428317701648.
24. Chung IH, Lu PH, Lin YH, Tsai MM, Lin YW, Yeh CT, et al. The long non-coding RNA LINC01013 enhances invasion of human anaplastic large-cell lymphoma. Sci Rep. 2017;7:295.
25. Huang PS, Chung IH, Lin YH, Lin TK, Chen WJ, Lin KH. The Long non coding RNA MIR503HG enhances proliferation of human ALK-negative anaplastic large-cell lymphoma. Int J Mol Sci. 2018; 19:1463.
26. Fragliasso V, Chiodo Y, Ferrari-Amorotti G, Soliera AR, Manzotti G, Cattelani S, et al. Phosphorylation of serine 21 modulates the proliferation inhibitory more than the differentiation inducing effects of C/EBPalpha in K562 cells. J Cell Biochem. 2012;113:1704–13.
27. Sancisi V, Manzotti G, Gugnoni M, Rossi T, Gandolfi G, Gobbi G, et al. RUNX2 expression in thyroid and breast cancer requires the cooperation of three non-redundant enhancers under the control of BRD4 and c-JUN. Nucleic Acids Res. 2017;45:11249–67.
28. Gugnoni M, Sancisi V, Gandolfi G, Manzotti G, Ragazzi M, Giordano D, et al. Cadherin-6 promotes EMT and cancer metastasis by restraining autophagy. Oncogene. 2016;36:667.
29. Verma A, Jiang Y, Du W, Fairchild L, Melnick A, Elemento O. Transcriptome sequencing reveals thousands of novel long noncoding RNAs in B cell lymphoma. Genome Med. 2015;7:110.
30. Fededa JP, Gerlich DW. Molecular control of animal cell cytokinesis. Nat Cell Biol. 2012;14:440–7.
31. Herriges MJ, Swarr DT, Morley MP, Rathi KS, Peng T, Stewart KM, et al. Long noncoding RNAs are spatially correlated with transcription factors and regulate lung development. Genes Dev. 2014;28:1363–79.
32. Werner MS, Sullivan MA, Shah RN, Nadadur RD, Grzybowski AT, Galat V, et al. Chromatin-enriched lncRNAs can act as cell-type specific activators of proximal gene transcription. Nat Struct Mol Biol. 2017;24:596–603.
33. Engreitz JM, Ollikainen N, Guttman M. Long non-coding RNAs: spatial amplifiers that control nuclear structure and gene expression. Nat Rev Mol Cell Biol. 2016;17:756.
34. Geiman TM, Muegge K. Lsh, an SNF2/helicase family member, is required for proliferation of mature T lymphocytes. Proc Natl Acad Sci USA. 2000;97:4772–7.
35. Tao Y, Liu S, Briones V, Geiman TM, Muegge K. Treatment of breast cancer cells with DNA demethylating agents leads to a release of Pol II stalling at genes with DNA-hypermethylated regions upstream of TSS. Nucleic Acids Res. 2011;39:9508–20.
36. Tao Y, Xi S, Briones V, Muegge K. Lsh mediated RNA polymerase II stalling at HoxC6 and HoxC8 involves DNA methylation. PLoS ONE. 2010;5:e9163.
37. Thijssen PE, Ito Y, Grillo G, Wang J, Velasco G, Nitta H, et al. Mutations in CDCA7 and HELLS cause immunodeficiency-centromeric instability-facial anomalies syndrome. Nat Commun. 2015;6:7870.
38. von Eyss B, Maaskola J, Memczak S, Mollmann K, Schuetz A, Loddenkemper C, et al. The SNF2-like helicase HELLS mediates E2F3-dependent transcription and cellular transformation. EMBO J. 2012;31:972–85.
39. Xi S, Zhu H, Xu H, Schmidtmann A, Geiman TM, Muegge K. Lsh controls Hox gene silencing during development. Proc Natl Acad Sci USA. 2007;104:14366–71.
40. Orom UA, Shiekhattar R. Long noncoding RNAs usher in a new era in the biology of enhancers. Cell. 2013;154:1190–3.
41. Wang R, Shi Y, Chen L, Jiang Y, Mao C, Yan B, et al. The ratio of FoxA1 to FoxA2 in lung adenocarcinoma is regulated by LncRNA HOTAIR and chromatin remodeling factor LSH. Sci Rep. 2015;5:17826.
42. Pizzi M, Margolskee E, Inghirami G. Pathogenesis of Peripheral T Cell Lymphoma. Annu Rev Pathol. 2018;13:293–320.
43. Zeng Y, Feldman AL. Genetics of anaplastic large cell lymphoma. Leuk Lymphoma. 2016;57:21–27.
44. Nobili L, Ronchetti D, Taiana E, Neri A. Long non-coding RNAs in B-cell malignancies: a comprehensive overview. Oncotarget. 2017;8:60605–23.
45. Lee CS, Ungewickell A, Bhaduri A, Qu K, Webster DE, Armstrong R, et al. Transcriptome sequencing in Sezary syndrome identifies Sezary cell and mycosis fungoides-associated lncRNAs and novel transcripts. Blood. 2012;120:3288–97.
46. Piva R, Agnelli L, Pellegrino E, Todoerti K, Grosso V, Tamagno I, et al. Gene expression profiling uncovers molecular classifiers

for the recognition of anaplastic large-cell lymphoma within peripheral T-cell neoplasms. J Clin Oncol. 2010;28:1583–90.
47. Huynh J, Etemadi N, Hollande F, Ernst M, Buchert M. The JAK/STAT3 axis: a comprehensive drug target for solid malignancies. Semin Cancer Biol. 2017;45:13–22.
48. Zamo A, Chiarle R, Piva R, Howes J, Fan Y, Chilosi M, et al. Anaplastic lymphoma kinase (ALK) activates Stat3 and protects hematopoietic cells from cell death. Oncogene. 2002;21:1038–47.
49. Rastogi P, Deva AK, Prince HM. Breast Implant-associated anaplastic large cell lymphoma. Curr Hematol Malig Rep. 2018;13:516–24.
50. Kucuk C, Jiang B, Hu X, Zhang W, Chan JK, Xiao W, et al. Activating mutations of STAT5B and STAT3 in lymphomas derived from gammadelta-T or NK cells. Nat Commun. 2015;6:6025.
51. Hammaren HM, Virtanen AT, Raivola J, Silvennoinen O. The regulation of JAKs in cytokine signaling and its breakdown in disease. Cytokine. 2019;118:48–63.
52. Fan C, Tang Y, Wang J, Xiong F, Guo C, Wang Y, et al. Role of long non-coding RNAs in glucose metabolism in cancer. Mol Cancer. 2017;16:130.
53. Debidda M, Wang L, Zang H, Poli V, Zheng Y. A role of STAT3 in Rho GTPase-regulated cell migration and proliferation. J Biol Chem. 2005;280:17275–85.
54. Teng TS, Lin B, Manser E, Ng DC, Cao X. Stat3 promotes directional cell migration by regulating Rac1 activity via its activator betaPIX. J Cell Sci. 2009;122:4150–9.
55. Lungu C, Muegge K, Jeltsch A, Jurkowska RZ. An ATPase-deficient variant of the SNF2 family member HELLS shows altered dynamics at pericentromeric heterochromatin. J Mol Biol. 2015;427:1903–15.
56. Han Y, Ren J, Lee E, Xu X, Yu W, Muegge K. Lsh/HELLS regulates self-renewal/proliferation of neural stem/progenitor cells. Sci Rep. 2017;7:1136.
57. Zhang G, Dong Z, Prager BC, Kim LJ, Wu Q, Gimple RC, et al. Chromatin remodeler HELLS maintains glioma stem cells through E2F3 and MYC. JCI Insight. 2019;4:e126140.
58. He X, Yan B, Liu S, Jia J, Lai W, Xin X, et al. Chromatin remodeling factor LSH drives cancer progression by suppressing the activity of fumarate hydratase. Cancer Res. 2016;76:5743–55.
59. Behan FM, Iorio F, Picco G, Goncalves E, Beaver CM, Migliardi G, et al. Prioritization of cancer therapeutic targets using CRISPR-Cas9 screens. Nature. 2019; 568:511–16.